Study of Laser-Hole Boring into Overdense Plasmas

R. Kodama,[1] K. Takahashi,[1] K. A. Tanaka,[2] M. Tsukamoto,[3] H. Hashimoto,[1] Y. Kato,[1] and K. Mima[1]
[1]*Institute of Laser Engineering, Osaka University, Yamada Oka 2-6 Suita, Yamada Oka, Osaka 565, Japan*
[2]*Department of Electromagnetic Energy Engineering, Osaka University, Yamada Oka 2-1 Suita, Osaka 565, Japan*
[3]*Welding Research Institute, Osaka University, 11-1 lbaraki, Mihogaoka, Osaka 567, Japan*
(Received 17 May 1996)

Laser channeling into an overdense plasma was studied using time-resolved spectra of a backscattered laser light. A 1053 nm laser light was focused on a preformed plasma at a laser intensity of 2×10^{17} W/cm^2 with a pulse duration of 100 psec. The preformed plasma was created with a 100-μm plastic target irradiated by 351-nm laser lights. Temporal profiles of the backscattered light and the angular distribution of scattered light indicate laser-hole boring in the preformed plasma. The x-ray pinhole images and strong redshift of the backscattered light spectrum are consistent with the channel formation into an overdense region. [S0031-9007(96)01815-7]

PACS numbers: 52.35.Mw, 52.40.Nk, 52.50.Jm

Studies of laser channeling into overdense plasmas are essential for the fast ignitor concept in inertial confinement fusion. In this concept, an ultraintense laser light penetrates into and ignites a highly compressed fuel core plasma [1]. Prechanneling or hole boring may be required to transport efficiently the ignitor pulse into the overdense region close to the core plasma. A prepulse laser light with a long duration (a few tens of ps to 100 ps) at intensities $I_L\lambda^2$ of 10^{17} to 10^{18} W μm^2/cm^2 must be focused to create a prechannel into overdense regions, where λ is the laser wavelength and I_L is the laser intensity. At these intensities, electron quiver motions dominate thermal motions. In a long-scale inhomogeneous plasma, the ponderomotive force will evacuate the underdense plasma radially and push the critical surface forward, resulting in the laser channel formation into overdense plasmas [2]. Once the channel is created in the plasma with a critical density, the laser light absorption [3] and nonlinear instability [4–6] are affected by density steepening near the critical density at the front of the channel. Substantial studies were performed on filamentations and channeling in underdense plasmas [7–12] and in overdense plasmas with a psec-laser pulse [13,14]. However, no experimental work has been reported so far on laser channeling into an overdense plasma at laser intensities of $>10^{17}$ W/cm^2 with pulse durations above a few tens of psec. In this paper, we present a study of channeling of a 1053 nm light into an overdense preformed plasma at an intensity of 2×10^{17} W/cm^2 and a pulse duration of 100 ps. The time-resolved backscattered light spectra and the angular distribution of the scattered light were obtained to study the dynamics of the light reflection point. We also took UV pictures probing the density perturbation at an underdense plasma and x-ray pictures for the channel formation into an overdense region.

The experiment was carried out using the GEKKO XII laser system at the Institute of Laser Engineering, Osaka University [15]. A CH plastic plane target with a thickness of 100 μm was irradiated obliquely by two 351-nm laser beams (5 J $\times$ 2) to produce a preplasma with a 300-μm focal spot at 50° incidence angles to the normal. A 1053-nm laser light as a main interaction pulse was focused normally onto the preplasma with an $f/3$ aspherical lens after 0.9 ns of the prepulse. The intensity of the main pulse was 2×10^{17} W/cm^2 at the best focus with a 30-μm spot diameter. The spot diameter of the best focus was estimated from x-ray images. All the pulse shapes were a Gaussian profile with a 100 psec full width at the half maximum (FWHM). The main laser focal positions were varied from 100 to 400 μm from the plastic target surface. The focus lens had a 30-μm spot size with approximately 160-μm depth of focus ($\pm$80 μm). The intensity at n_c was 2×10^{17} W/cm^2 for the 100–250-μm focus conditions and 3×10^{16} W/cm^2 for the 400-μm focus based on a density profile obtained by 1D hydrodynamic simulation. An ultraviolet probe laser system (263 nm and 10 ps) was used to monitor the created plasma shape using grid image refractometry (GIR) [16]. The GIR picture [17] showed a hole on the preplasma where the main laser was focused. The diffraction of the probe beam in the plasma limited the measured density to be about 3×10^{20}/cm^3. The position of this density region ($3 \pm 2 \times 10^{20}$/cm^3) without the main laser pulse was about 200 $\pm$ 20 μm from the target surface on the center axis, which was consistent with the simulation. X-ray images for a 1 to 30 keV x-ray range were monitored with x-ray CCD pinhole camera systems with a spatial resolution of 15 μm. The fraction of the backscattered light was measured with a calibrated biplaner photo diode. Time-resolved spectra of the backscattered light was measured with a 1/4 m spectrometer coupled to an S-l streak camera. The covered spectra were from 1050 to 1070 nm with a flat spectral response at a spectral resolution of 0.4 nm. The temporal resolution of the system was 13 psec limited by the width of a streak camera slit and spectral resolution. Estimation of the ion expulsion time in the focal spot (30 μm diam) using an equation of motion [9,18] is about a few ps to 20 ps. A thermal pressure is neglected in this estimation

 0031-9007/96/77(24)/4906(4)$10.00

since the quiver energy is 20–40 times larger than the thermal energy at 1 keV. This time scale is comparable to the time resolution of diagnostics (13 ps). The dynamics of the observed spectra could be affected by the ion motion.

Figure 1 shows typical streak camera images of the backscattered spectra at focus positions of (a) 100 μm and (b) 250 μm from the target surface. As a common feature in all the focus conditions, a 2–3 nm blueshift from the fundamental (1053 nm) was observed at 100 ps prior to the pulse peak. This blueshift was observed only early in time of the pulse and rapidly shifted to the red side in time. However, no such blueshift was observed when the pulse was focused on the target surface without a preplasma. This initial blueshift is due to the Doppler shift caused by the expansion of the preplasma since this blueshift $\Delta\lambda_b$ is dependent on the prepulse laser intensity as $\Delta\lambda_b \sim I_L^{0.18-0.29}$ at intensities of $(0.4-5) \times 10^{14}$ W/cm^2. The magnitude of the Doppler shift indicates preplasma expansion speeds of $(2.5-4.0) \times 10^7$ cm/s at a prepulse intensity of 1.4×10^{14} W/cm^2. As spectral peak was shifted to the red side and the shape changed in time, there is a difference in the redshifts depending on the focus positions. The peaks of the redshifts from the fundamental wavelength were 1–2 nm at a focus position of 100 μm, 5–6 nm at 250 μm, and 6–7 nm at 400 μm, which changed gradually in time. The long wavelength cutoff $\Delta\lambda_c$ also shows a clear dependence on the focus position. The temporal change in the spectral shift $\Delta\lambda_c/\Delta t$ may be relevant to the speed (V) of the reflection point as $\Delta\lambda_c/\Delta t \propto V$. The $\Delta\lambda_c/\Delta t$ for the 250 μm and the 400 μm focus are 1.5 to 2 times larger than that for the 100 μm. The dynamics of the spectra may indicate that the reflection points for the 250 μm and the 400 μm focus are accelerated much faster than that for the 100 μm focus. Laser hole boring might be affected by the focusing point if the spectra was caused by the reflection from the front edge of the hole.

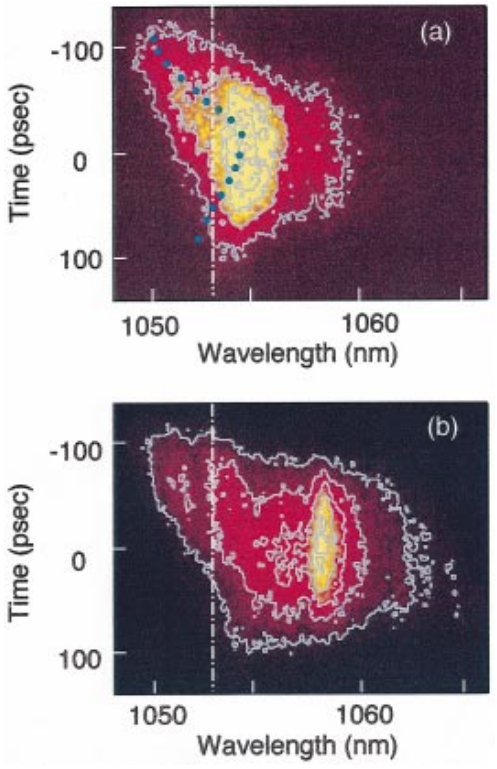

FIG. 1(color). Linear intensity contours of the time-resolved spectra of the backscattered light at the focus positions of (a) 100 μm and (b) 250 μm. The dotted lines correspond to the fundamental wavelength. The closed circles in (a) are estimations of Doppler shifts due to critical surface moving inward by the photon pressure.

The spectra at the pulse peak varying the focus position are shown in Fig. 2. The dotted line in Fig. 2(a) is the spectrum without the preplasma, focusing the beam on the target surface at 2×10^{17} W/cm^2. The spectral peak intensity of the backscattered light without the preplasma was lower than those with the preplasma, consistent with the angular dependence of the scattered light as described later. The spectrum without the preplasma was simply broadened to the red side with a spectral width of about 2.2 nm. Totally different spectra were observed as the main pulse interacted with the preplasma. The spectra from the preplasma consist of a strong redshifted and a weak broad components. Spectral broadening of the base component could be influenced by the strongly coupled stimulated Brillouin scatter (SBS) instability since the growth rate γ_0 is larger than the ion acoustic wave frequency ω_{ia} at 2×10^{17} W/cm^2, satisfying the strong coupling condition as $\gamma_0/\omega_{ia} \sim 10$ at $0.2n_c$ for 1 keV [19]. However, it might be difficult to explain the redshifted component only by the strongly coupled SBS. Changing

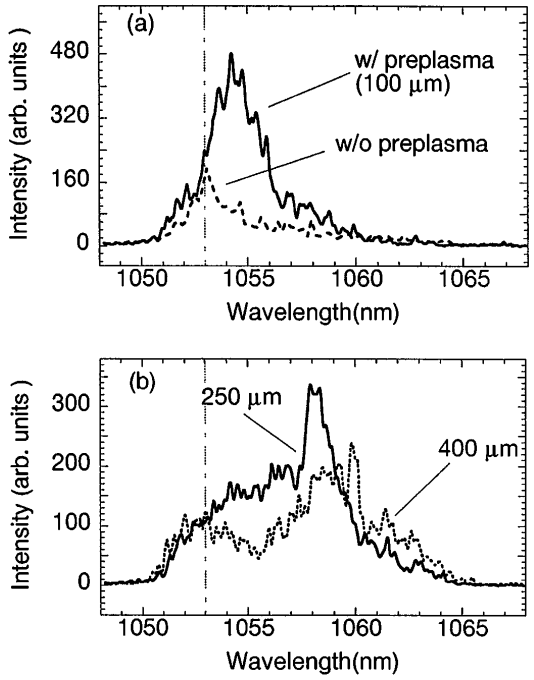

FIG. 2. The backscattered spectra at the pulse peak for the (a) 100 μm focus, (b) 250 and 400 μm focus. The dotted line in (a) is the spectra without the preplasma.

the focus condition, the spectral width and the peak intensity of the redshifted component decrease with the spectral shift $\Delta\lambda_r$ to the red side. The width and the relative peak intensity for the 100 μm focus were 2.5 nm and 460 counts ($\Delta\lambda_r = 1-2$ nm), 1.3 nm and 300 counts for the 250 μm ($\Delta\lambda_r = 5-6$ nm), and 0.5 nm and 200 counts for the 400 μm ($\Delta\lambda_r = 6-7$ nm). The spectral narrowing and reduction of the peak intensity as the redshift increases may indicate the reduction of SBS with density steepening by the ponderomotive force in laser-hole boring [4,6].

Temporal history of the backscattered light showed the saturation of the reflectivity at around the laser pulse peak. Increasing the laser intensity by one order of magnitude (10^{16} to 10^{17} W/cm^2) in time, the reflectivity decreased by a factor of about 2. It is difficult to explain this reduction only by the saturation of SBS due to the transition to the strong couple limit because the γ_0 is already comparable to the ω_{ia} at intensities of 10^{15} W/cm^2 for 1 keV and 10^{16} W/cm^2 for 5 keV at $0.01n_c$ for a homogeneous plasma. As a consequence of the hole in the plasma, the SBS reflectivity may be limited by density steepening [4]. The resonant absorption on the wall is also an important process in the hole [3]. The absorption due to $\mathbf{J} \times \mathbf{B}$ heating may continue at the deepest part of the hole [20]. The increase in the absorption and/or the reduction of SBS in the hole could decrease the reflectivity. Applying this absorption dependence in the hole to the experimental results, the reduction of the reflectivity with the laser intensity in the pulse is consistent with the property of the redshift component (spectral narrowing and decrease in the peak intensity with the amount of the redshift) changing the focus position. As we discuss later, the backscattered light might indicate that a hole boring was formed more clearly for the 250 μm and the 400 μm focus that the 100 μm focus.

The angular distribution of the scattered light was monitored at angles of 0° ± 10°, 30° ± 1°, and 47.5° ± 1°, and is shown in Fig. 3. The spectral response of the scattered light measurements was the same as that of the backscattered light measurement. The angular dependence of the scattered light without a preplasma is assumed as cosine^2 distribution [21] because of no relative calibration of the detectors to each channel. This assumption should be appropriate for the qualitative discussion of the angular distribution of the scattered light. The distribution was clearly collimated to back side as cosine^{12} when the main laser was injected into the preplasma, indicating a channel formation in the preplasma.

X-ray pictures from different observation angles for the 250 μm focus are shown in Fig. 4. A spot size on the target surface geometrically determined by the focus cone was >80 μm, represented as dotted lines in the figure. A weak spot with a 300 μm diam was due to the preformed plasmas. A strong tight spot of <30 μm on the target surface was observed only for the 250 μm focus, and no such tight spot was obtained for the 100 μm and the 400 μm focus. If the tight spot on the target surface was caused by the electrons transported from the critical density point, the similar spot should appear at other focus conditions. Taking account of the aspect ratio of the spot size (about 30 μm diam) to the distance from the critical density point to the target surface (100–150 μm), it is also difficult to explain the hot spot with thermal electrons which could be diffusively transported (2D effect).

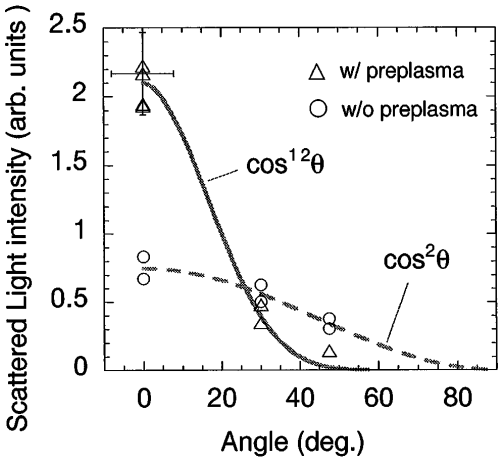

FIG. 3. The angular distribution of the scattered light at the focus positions of 0 μm for no preplasma and 200 ± 50 μm for the preplasma from the target surface.

Assuming the redshift as shown in Fig. 1 is a Doppler shift due to the critical surface moving inward by the photon pressure, e.g., 60 Mbar at 10^{17} W/cm^2, the propagation distance of the critical surface is of the order of 20 μm for the 100 μm focus. The distance for the 250 μm focus was 120 μm, close to the distance between the initial critical and the target surfaces. The Doppler shift was evaluated from a simple snow plow model calculation (1D) with momentum balance between the photon pressure and mass

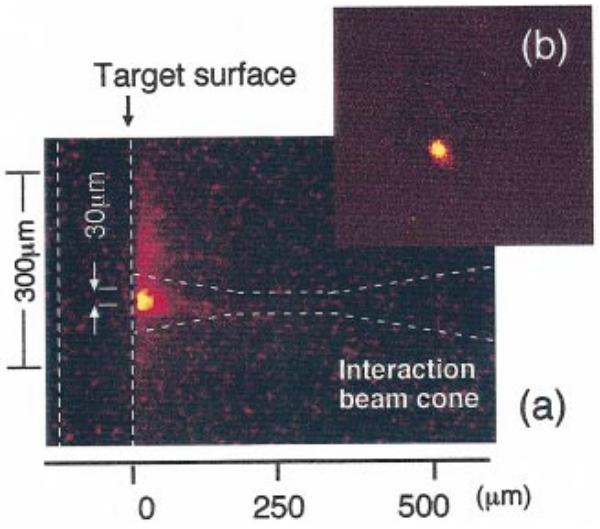

FIG. 4(color). X-ray pinhole camera images from (a) the target tangential and (b) 10° to the target normal. The dotted line shows a cone of the incident laser light at 250 μm from the target surface.

flow at the critical surface by using a preformed plasma density profile from 1D simulation and a 100 ps (FWHM) Gaussian profile of the laser pulse. This estimated value is close to the measured redshift for the 100 μm, shown as a dotted line in Fig. 1(a). However, a laser intensity of 2×10^{18} W/cm^2, where the relativistic self-focusing become an important factor, may be necessary to yield a Doppler shift as large as 5 nm to move the critical point. The x-ray image showing the tight spot on the target surface, obtained only for the 250 μm, is consistent with the strong redshift (5 nm) of the backscattered light if a whole beam channel is self-focused into the overdense region close to the target surface.

Required critical power for sustaining of a stable channel can be estimated in an underdense homogeneous plasma within a sufficiently short time duration. Calculation taking account of the relativistic and charge-displacement mechanisms shows that a critical power given by $P_c = 16(\omega/\omega_p)^2$ GW is required to overcome classical diffraction [7]. This critical power may be applied for the experimental conditions early in time of the pulse (a few psec), where the ion motion can be ignored, corresponding to the laser intensity of 10% of the peak (0.1–0.15 TW). This laser intensity ($P_L = 0.15$ TW) exceeds the critical power by factors of 1 to 5 at $0.1n_c$ to $0.6n_c$, the stable region of which are located at about 150 to 300 μm from the target surface. For the 250-μm focus, the focal depth is located in this stable region with $P_c < P_L < 5P_c$. To create a stable channel, the laser beam should be focused onto the edge of the stable region [7,8]. This condition may be consistent with the backscattered light spectra implying formation of a channel for the 250-μm focus. However, the 100-μm case corresponding to the beam focus interior to this stable region may lead to distortion of the incoming laser beam and inhibit self-focusing. For the 400 μm focus, the backscattered light shows the spectral modulation, implying the beam spreading or breaking into filaments. No observation of a tight spot on the x-ray image for the 400-μm focus might be also due to the beam spreading before directly reaching of the laser beam onto the target surface. At $0.6n_c$ to n_c, $5P_c < P_L < 10P_c$, where the stable channeling could be transitive to filamentation [7]. The distance from the interior edge of the focal depth to the original critical density point is about 170–220 μm for the 400-μm focus, whereas the distance for the 250-μm focus is about 20–70 μm. A theoretical filamentation growth length for a homogeneous plasma is about 60–170 μm at 0.1–$0.01n_c$ with 10% of the laser peak intensity for 1 keV [11,22]. Thus the channel could be broken into filaments and stopped before reaching of the beam onto the target surface [6,23].

There are several mechanisms as other possibilities to explain the backscattered spectra as shown in Fig. 1. One of them might be strong coupled stimulated Raman scattering (SRS). Short laser pulse (sub psec) experiments on the strong coupled SRS show unusually shifted spectra at around the fundamental wavelength [24]. However, all the short pulse experiments used homogeneous low density plasmas, e.g., $n_e < 1/100n_c$. In our experiment the preplasma has an exponential profile with overdense to solid densities and the best focus was placed at near the critical density surface. No strong effect will be expected on the SRS region changing the focus position in our experimental condition.

In conclusion, we have measured time-resolved spectra of the backscattered light from an inhomogeneous preformed plasma interacting with a 1053 nm laser light at 2×10^{17} W/cm^2 with a 100 ps pulse. The UV probe image, the temporal profiles of the backscattered light, and the angular distribution of scattered light indicate laser-hole boring in the preplasma. The x-ray pinhole images and the strong redshift of the backscattered light imply self-focusing and subsequent laser channeling up to a solid density.

We acknowledge all the technical support of the engineering staff at the Institute of Laser Engineering for the laser system operation, target fabrication, and data acquisition. We would like to thank Dr. P. E. Young and Dr. K. Mizuno, Lawrence Livermore National Laboratory, for usefull discussions.

[1] M. Tabak *et al.,* Phys. Plasmas. **1**, 1626 (1994).
[2] S. C. Wilks, Phys. Fluids B **5**, 2603 (1993).
[3] F. Brunel, Phys. Fluids **31**, 2714 (1988); Phys. Rev. Lett. **59**, 52 (1987).
[4] W. E. Kruer *et al.,* Phys. Rev. Lett. **35**, 1076 (1975).
[5] M. R. Amin *et al.,* Phys. Fluids B **5**, 3748 (1993).
[6] V. V. Eliseev *et al.,* Phys. Plasmas **2**, 1712 (1995); K. A. Tanaka *et al.,* Phys. Fluids **28**, 2910 (1985).
[7] A. B. Borisov *et al.,* Phys. Rev. Lett. **65**, 1753 (1990); **68**, 2309 (1992); A. B. Borisov *et al.,* Phys. Rev. A **45**, 5830 (1992).
[8] P. Monot *et al.,* Phys. Rev. Lett. **74**, 2953 (1995).
[9] W. B. Mori *et al.,* Phys. Rev. Lett. **60**, 1298 (1988).
[10] P. E. Young *et al.,* Phys. Rev. Lett. **63**, 2812 (1989); P. E. Young *et al.,* Phys. Rev. Lett. **75**, 1082 (1995).
[11] P. E. Young *et al.,* Phys. Plasmas **2**, 2825 (1995).
[12] S. Wilks *et al.,* Phys. Rev. Lett. **73**, 2994 (1994).
[13] X. Lui and D. Umstadter, Phys. Rev. Lett. **69**, 1935 (1992).
[14] M. P. Kalashnikov *et al.,* Phys. Rev. Lett. **73**, 260 (1994).
[15] K. Takahashi *et al.,* Prog. Cryst. Growth Charact. **33**, 273 (1996).
[16] R. S. Craxton *et al.,* Phys. Fluids B **5**, 4419 (1993).
[17] K. Takahashi *et al.,* ILE Research Report No. ILE-9603P, 1996 (unpublished).
[18] W. E. Kruer, *The Physics of Laser Plasma Interactions* (Addison-Wesley, Redwood City, California 1988).
[19] D. W. Forslund *et al.,* Phys. Fluids **18**, 1002 (1975); P. E. Young *et al.,* Phys. Rev. Lett. **73**, 2051 (1994); S. D. Baton *et al.,* Phys. Rev. E **49**, R3602 (1994).
[20] W. E. Kruer, and K. Estabrook, Phys. Fluids **28**, 430 (1985).
[21] L. M. Goldman *et al.,* Phys. Rev. Lett. **31**, 1184 (1973); B. H. Ripin *et al.,* Phys. Rev. Lett. **33**, 634 (1974).
[22] P. L. Kelley, Phys. Rev. Lett. **15**, 1005 (1965).
[23] P. E. Young *et al.,* Phys. Rev. Lett. **61**, 2336 (1988).
[24] C. B. Darrow *et al.,* Phys. Rev. Lett. **69**, 442 (1992).